Peer Community Journal

Section: Ecology

Research article

Published
2025-05-05

Cite as
Mirjam R Rieger, Christoph Grüneberg, Michael Oberhaus, Sven Trautmann, Madalin Parepa and Nils Anthes (2025) *Bird population trend analyses for a monitoring scheme with a highly structured sampling design*, Peer Community Journal, 5: e45.

Correspondence
nils.anthes@uni-tuebingen.de

Peer-review
Peer reviewed and recommended by PCI Ecology, https://doi.org/10.24072/pci.ecology.100748

Bird population trend analyses for a monitoring scheme with a highly structured sampling design

Mirjam R Rieger [1], Christoph Grüneberg [2], Michael Oberhaus [2], Sven Trautmann [3], Madalin Parepa [1], and Nils Anthes [1]

Volume **5** (2025), article e45

https://doi.org/10.24072/pcjournal.550

Abstract

Population trends derived from systematic monitoring programmes are essential to identify species of conservation concern and to evaluate conservation measures. However, monitoring data pose several challenges for statistical analysis, including spatial bias due to an unbalanced sampling of natural regions or habitats, variation in observer expertise, frequent observer changes, and overdispersion or zero-inflation in the raw data. An additional challenge arises from so-called 'rolling' survey designs, where each site is only visited once within each multi-year rotation cycle. We developed a GAMM-based workflow that addresses these challenges and exemplify its application with the highly structured data from the Ecological Area Sampling (EAS) in the German federal state North Rhine-Westphalia (NRW). First, we derive a routine that allows informed decisions about the most appropriate combination of distribution family (Poisson or negative binomial), model covariates (e.g., habitat characteristics), and zero-inflation formulations to reflect species-specific data distributions. Second, we develop a correction factor that buffers population trend estimates for variation in observer expertise as reflected in variation in total bird abundance. Third, we integrate region-specific trends that adjust for between-year variation in the representation of habitat or natural regions within the yearly subset of sampled sites. In a consistency check, we found good match between our GAMM-based EAS trends and TRIM-based trends from the German Common Bird Monitoring scheme. The study provides a template script for *R* statistical software so the workflow can be adapted to other monitoring programmes with comparable survey designs and data structures.

[1]Institute of Evolution and Ecology, University of Tübingen, Auf der Morgenstelle 28, 72076 Tübingen, Germany, [2]State Agency for Nature, Environment and Climate in North Rhine-Westphalia (LANUK), 40208 Düsseldorf, Germany, [3]Dachverband Deutscher Avifaunisten e.V., An den Speichern 2, 48147 Münster, Germany

Peer Community Journal is a member of the Centre Mersenne for Open Scientific Publishing
http://www.centre-mersenne.org/

e-ISSN 2804-3871

Introduction

Bird populations decline worldwide (Klvaňová et al., 2009; Sauer et al., 2017; Burns et al., 2021), with the European Union alone facing an approximate loss of 560–620 million bird individuals (17–19%) within 40 years (Burns et al., 2021). Such knowledge of population sizes and their trends heavily relies on standardised monitoring programmes to provide reliable population density estimates. The resultant population trend estimates allow allocating conservation resources to species of highest conservation concern (Niemelä, 2000; Buckland & Johnston, 2017), provide feedback on the efficiency of conservation efforts (Johnston et al., 2015), and raise awareness for the value and state of biodiversity among decision makers and the public (Jennings, 2021).

However, many monitoring programmes pose substantial challenges for statistical inference that can reduce the reliability and robustness of the estimated trends if not treated with care (Buckland & Johnston, 2017). Our study focuses on a monitoring scheme with a rolling (or 'rotating') survey design that generates multi-year intervals between repetitive surveys per site (Buckland & Johnston, 2017). Rolling surveys can cover more study sites and thus a wider range of habitats or natural regions across years than monitoring schemes with a yearly coverage of all sites but result in a large fraction of sites with missing values each year and frequent observer changes. In this context, we develop an analytical protocol to cover three core aspects. First, rolling monitoring programmes rest on spatially structured sampling designs, often coupled with between-year variation in the representation of habitat types, which needs integration into the analysis (van Strien et al., 2004; Buckland & Johnston, 2017). Spatial bias arises when relevant natural regions or habitats are not represented according to their spatial coverage in the monitoring sample (van Strien et al., 2004). As a result, when population trends vary between natural regions or habitats, the estimated overall population trend can be biased towards overrepresented natural regions, or reflect changes in sample composition rather than a true change in abundance (Buckland & Johnston, 2017; Bowler et al., 2022).

Second, detection probabilities and survey quality can vary strongly among and (over time) within observers, potentially introducing random and systematic trend estimation errors when ignored (Sauer et al., 1994; Link & Sauer, 1998; Kéry et al., 2005; Jiguet, 2009; Farmer et al., 2014). When average observer expertise remains constant, between-observer variation primarily increases (random) variation in abundance estimates between sites and years (Sauer et al., 1994; Johnston et al., 2018). In contrast, within-observer learning and systematic changes in average observer expertise introduce (systematic) biases in trend estimates. For example, initial familiarisation with a new study site and the specificities of the monitoring programme usually cause underestimated bird abundances in early survey years (Link & Sauer, 1998; Jiguet, 2009). Moreover, observer expertise usually increases with time after active engagement in bird territory surveys, while species detectability declines with age if hearing impairment reduces the detection of high-pitch bird vocalisations (Farmer et al., 2014). In rolling survey design, these general issues typically go along with a high turnover in observer identities between successive surveys of the same site, which adds further variation.

Finally, count response data as typical for bird census require models to reflect distribution properties such as overdispersion or zero inflation (Blasco-Moreno et al., 2019; Campbell, 2021). Overdispersion arises when the variance of count data exceeds their mean value. It is typically resolved by modelling trends with a negative binomial error distribution instead of a Poisson distribution (Blasco-Moreno et al., 2019; Campbell, 2021). Zero-inflation occurs when datasets contain so-called structural zeros. This implies a disproportionally large fraction of unoccupied sites that cannot be explained solely by sampling variation among sites considered suitable, but rather arises from survey sites that are unsuitable. Where present, structural zeros are modelled separately from the count distribution in zero-inflated model components (Korner-Nievergelt et al., 2015; Blasco-Moreno et al., 2019; Campbell, 2021; Tirozzi et al., 2021).

The software TRIM (Pannekoek & van Strien, 2001) represents a common analytical tool for the analysis of monitoring data and is used, for example, in the Pan European Common Bird Monitoring Scheme (Vorisek et al., 2008) and the national bird monitoring programmes of Sweden (Jiguet et al., 2013), Finland (Pöysä et al., 2013), or Germany (Kamp et al., 2021). TRIM computes trends and annual population indices from loglinear Poisson regressions. It corrects for overdispersion, serial correlation and missing values and allows weights to account for spatial bias (van Strien et al., 2004). Yet, designed for monitoring schemes with almost yearly surveys per site by the same observer, TRIM estimates are considered robust unless the turnover in survey sites between years leads to a ≥ 60 % fraction of missing values (van Strien et al., 2001; Bogaart et al., 2020; Dakki et al., 2021). Moreover, TRIM is restricted to categorical covariates, requiring climate or landscape composition covariates to be transformed into categories (Bogaart et al., 2020). Finally, long-term trend analyses beyond yearly index estimates are restricted to linear trends and breakpoint analyses, while more recent developments favour the integration of trend smoothers, e.g. with general additive (mixed) models (GA(M)Ms) (e.g., Fewster et al. (2000); Knape (2016)). Using a smoothing function, GA(M)Ms can also capture non-linear short- and long-term trends while allowing to identify periods of strongly increasing or decreasing trends and breakpoints of (linear) trend direction (Fewster et al., 2000; Zuur, 2012; Knape, 2016; Wood, 2021).

We develop a user-friendly tool that integrates high observer turnover, long time gaps between successive surveys, spatial bias, as well as overdispersion and zero-inflation into an analysis of bird abundance trends from rolling surveys. It is exemplified with data from the Ecological Area Sampling (EAS), a monitoring programme of the German federal state North Rhine-Westphalia (NRW) with a six-year rolling sampling scheme. As a quality check, we compared the predicted population trends with West German trends derived from the German Common Bird Monitoring scheme (MhB) with yearly surveys per site. The statistical approach is provided as an *R* script (Rieger et al., 2025a) and package (Rieger, 2024) that can be adjusted to other datasets with a comparable structure.

Material and Methods

The Ecological area sampling (EAS) dataset

The Ecological Area Sampling (EAS) is a long-term biodiversity monitoring programme of the State Agency for Nature, Environment and Climate in North Rhine-Westphalia (LANUK, former LANUV) with 170 study sites that represent the average landscape of North Rhine-Westphalia (NRW) (LANUV, 2016b). Sites are distributed across six natural regions and two biogeographic regions (atlantic lowlands, continental highlands) (Figure 1) proportional to their spatial coverage. Another 21 metropolitan sites were added in 2011 to represent habitat characteristics of the Rhine-Ruhr metropolis region (Weiss & Schulze-Hagen, 2014). The program targets an alternating six-year cycle for successive surveys of a given site but could not yet strictly impose it given restructuring in the yearly balance of sites among natural and metropolitan regions (see section ‘Spatial bias’). The dataset for the survey period 2002-2020 typically covered 25 to 36 (max. 47) sites per year, two to four replicated surveys per site, and 614 surveys in total. Each site is visited at least nine times per sampling year (two to eight hours per date) between February and July with complete coverage of its 1 km² area (LANUV, 2016a). The repetitive surveys are used to derive the territory count per species and km², which represents the response variable *abundance* in all statistical analyses (LANUV, 2016a). Survey effort (survey number and duration) constitute relevant model covariates but the respective information is not available for the current dataset (Further detail on EAS methodology in Appendix 1).

Site characterisation

Sites were distributed into six natural regions and whether they were located in a metropolitan area or not (Figure 1). We combined these two layers of information to produce a new *natural regions* variable with seven levels, all sites within the metropolitan area being classified as

"metropolitan area" while others were classified according to the natural region they belong to. Another site-specific categorical variable was *biogeographic region* (atlantic, continental). Natural regions showed near-complete separation between biogeographical regions, where the continental region encompasses the natural regions 'silicate hillside' and 'limestone hillside' and the Atlantic region the remaining five natural regions including the 'metropolitan area' (Figure 2 right). We therefore only considered *biogeographic region* in the post-modelling process (see section 'Population trends').

Quantitative site characteristics included *altitude* above sea level (ATKIS, 2013), ten parameters of *climate* and three of *landscape compositions* to account for variation in mean environmental attributes between the site subsets surveyed per year. Climate parameters included long-term spring and winter averages between 1981 and 2010 (CDC, 2010) of minimum, mean, and maximum temperatures, precipitation, and sunshine duration. Landscape composition variables were the coverages of forest, arable land, and settlements (ATKIS, 2013). Given substantial collinearity between these 14 attributes, we integrated their principal components (PC) with eigenvalues exceeding 1 into the statistical models (three PCs in our case; for details see Appendix 2).

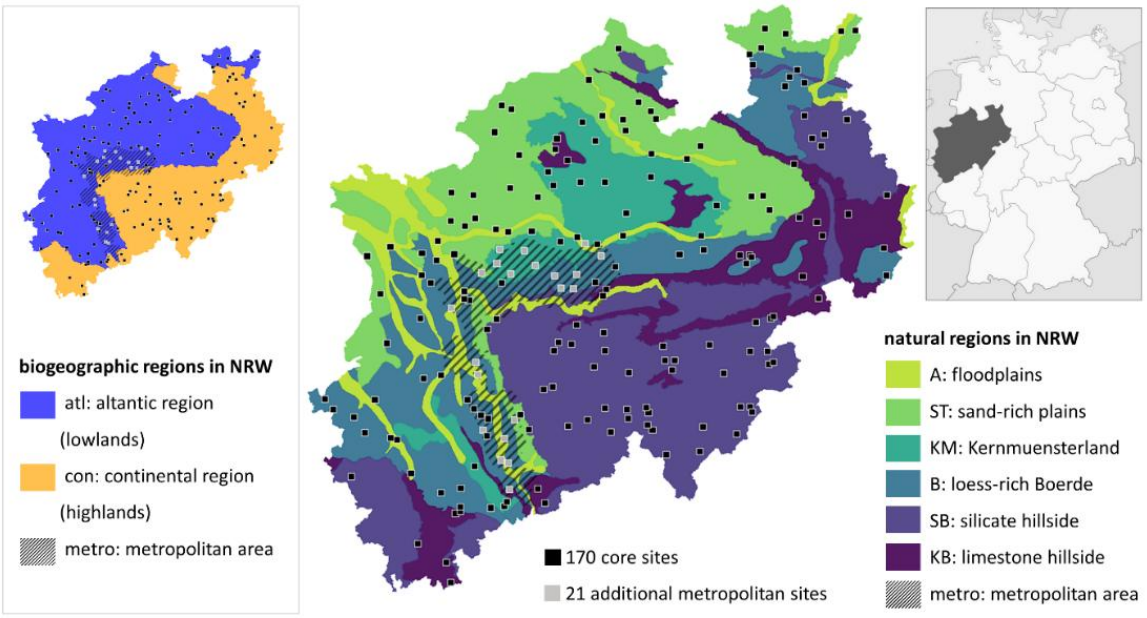

Figure 1 - Sites and study area of EAS coloured by six natural regions (middle) and two biogeographic regions (left), both including the Rhine-Ruhr metropolis, which was implemented as seventh natural region. Map adapted from LANUV (2016b).

Spatial bias

The initial sample of 170 EAS monitoring sites almost perfectly represented the proportional coverage of natural regions in NRW, but sampling bias arose from two sources. First, the monitoring programme added 21 metropolitan sites overrepresenting the metropolitan area to the other six natural regions in 2011. Second, the yearly subsampling of sites was highly unbalanced with respect to natural regions in the early phase of the EAS programme (Figure 2), with improvements since 2007 and almost perfect balance since 2013.

To account for the uneven allocation in early programme years and for the overrepresentation of metropolitan areas since 2011, we analysed annual trends per natural region.

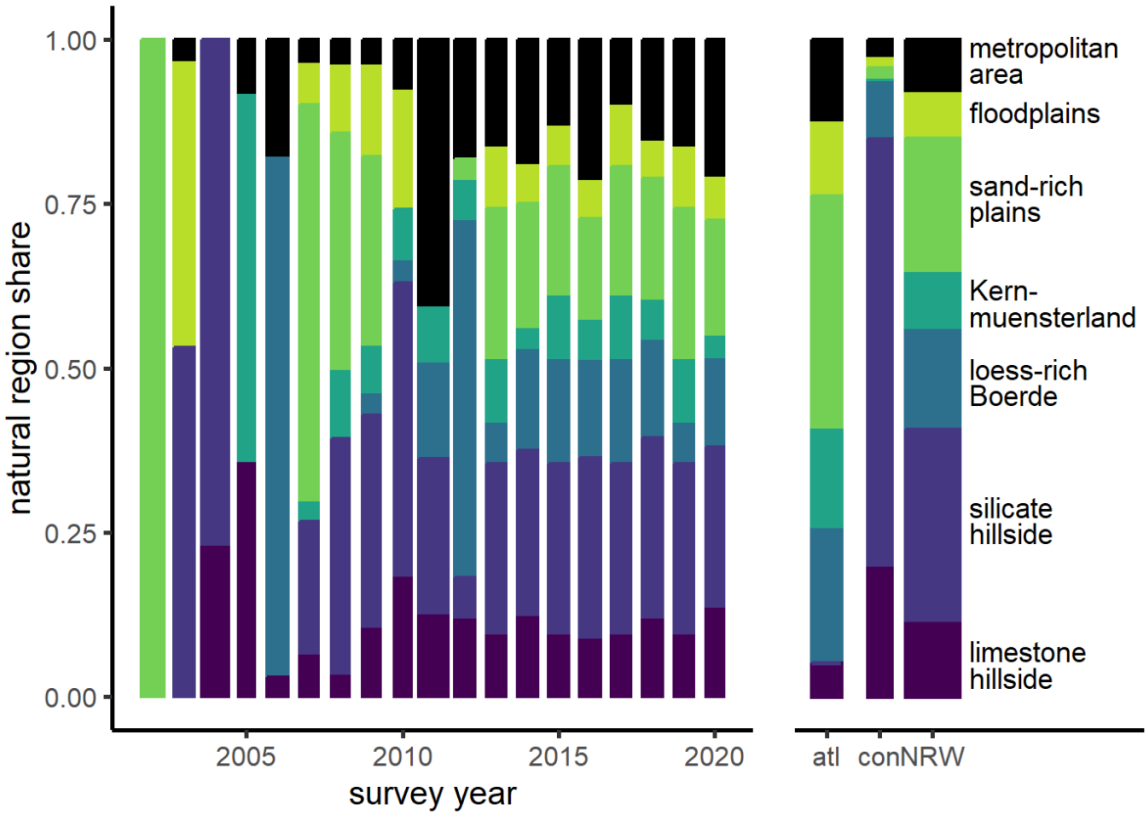

Figure 2 - Natural region shares in annual EAS samples (main panel) and their spatial coverage per biogeographic region (atlantic - atl, continental - con) and in NRW (right panel). Bar widths are proportional to the number of surveyed sites per year.

Observer effects

The delineation of breeding territories is prone to under- and overestimation arising from variation in observer expertise in species identification and detection, territory delineation, and general field survey quality (Südbeck et al., 2005; Johnston et al., 2018), even in programmes such as the EAS that hire skilled ornithologists (König, 2020). Observer effects add further noise to trend estimates when observers change between successive surveys of a given site. Excluding data from first year surveys, an established standard in monitoring data with yearly site coverage (e.g., German Common Bird Monitoring (Kamp et al., 2021)), is unfeasible for rolling surveys: In the EAS dataset, 434 out of 614 breeding bird surveys between 2002 and 2020 (71 %) were such first-year combinations of observer and site. To characterise observer expertise and learning effects, we therefore categorised observers as (i) unfamiliar with the survey programme and site, (ii) familiar with survey programme but unfamiliar with the site, or (iii) familiar with both. Yet, we excluded this predictor from final models since it did not improve model fit, most likely because site familiarisation introduced no detectable bias into the EAS trend estimates given the high observer turnover rates among successive surveys.

Instead, we identified surveys with suspiciously high or low territory counts summed across all species. The procedure assumes that severe observer effects typically manifest in a general under- or overestimation of territory numbers (= abundance), so that total abundance (summed across species) for a given site and year stands out against average total abundance for that site. Based on this logic, we calculated

(1) Observer effect = $\frac{N_{js}}{\overline{N_s}}$

with N_{js} the total abundance across species on site s in survey year j, and $\overline{N_s}$ the mean total abundance across species on site s across all survey years (Rieger, 2024). This observer effect is a ratio, so that a value of 1 indicates no deviation from the mean, and a value of 0.75 (1.25) a deviation of -25% (+25%) from the observed mean. We integrated the *observer effect* as a categorical predictor variable classified as 'negative' (or 'positive') when the abundance sum of a given survey was at least 25% smaller (or larger) than the mean per site, and as 'none' otherwise. As a sensitivity analysis, we also checked observer effect thresholds of 20% and 15%.

Distribution characteristics and the statistical analysis of EAS

We analysed species-specific abundance trends between 2002 and 2020 for all species with ≤ 90 % zero-sightings in both biogeographic regions (and thus at least 61 non-zero records) to allow plausible trend detection. The criterion was fulfilled in 61 (out of 148) species. For conciseness, this study focuses on a subset of 14 species that cover the observed range of abundance distributions and proportions of zero counts (Table 1).

Trends in *Abundance*, i.e. the territory count per site and year, were analysed using generalised additive mixed models (GAMMs) within a Bayesian framework as implemented in the package *brms* (v.2.21.0; (Bürkner, 2017) for R (v.4.3.3; (R Core Team, 2024). The *brms* package fits Bayesian models using *Stan* via the package *cmdstanr* (v.0.7.1; (Gabry & Češnovar, 2020) and allows to more flexibly integrate the required error families and model structures. We implemented four different error structures to account for zero-inflation or overdispersion, namely a Poisson error structure (Pois), negative binomial (nb), zero-inflated Poisson (zip), or zero-inflated negative binomial (zinb), all using a log link (Table 2, Appendix 3). Since the underlying survey method generates .5 abundances for peripheral territories, we multiplied *abundance* by two (so it would be number of territories for 2 km²) and added an *offset* of two to all models.

The main model was constructed as follows, and we explain each model component below:

(2) 2**Abundance* ~ s(*Year*, by = *Natural region*) + *Natural region* + *Observer* + poly(*PC1*, 2) + poly(*PC2*, 2) + poly(*PC3*, 2) + offset(log(2)) + (1|*siteID*)

Survey *Year* as the main continuous predictor was modelled with a smoothing function (thin plate regression splines with an automatic selection of the degree of smoothing and k = 10 default basis dimension, (Wood, 2021)) to account for non-linear changes in abundance over time while allowing adjacent years to be related to each other (Fewster et al., 2000; Zuur, 2012; Knape, 2016; Wood, 2021). Thus, smoothers buffer against the property of rolling surveys that sampled site subsets differ between successive years, so that year-to-year changes in abundance cannot differentiate among-site variation from true short-term change in population size (Zuur, 2012). Smoothers were modelled separately per *Natural region* to allow detecting regional differences in population trends and – for the overall trend estimates – accounting for spatial bias that may arise from unbalanced sampling design among regions (see above) in the post-modelling process (Figure 2).

We added *Natural region* as a categorical main effect (Wood, 2021) to contrast population densities and trends between the seven natural regions. Since natural regions showed near-complete separation between biogeographical regions (see Figure 2 right and section 'Site characterisation'), we therefore refrained from adding biogeographic region as a separate predictor, but extract population trends per biogeographic region by combining the respective natural region trends (see section 'Population trends').

Observer effects as outlined in section 'Observer effects' were added as a categorical covariate. For numeric covariates, we included linear and quadratic terms of site-specific environmental attributes captured in the first *three principal components PC1* to *PC3* as outlined in section 'Site characterisation' and Appendix 2. Finally, we added *site-ID* as a random intercept to reflect repeated measures per site and to model variation in mean abundance between the different site subsets per year.

The zero-inflation model component, where needed (Table 1), represents a binomial (Bernoulli) model with a logit link to estimate the additional occurrence of structural zeros. We kept this component as simple as possible (formulation 3) and estimated separate zero-inflation parameters per *Natural region*, environmental *PC*, or study *site-ID* (formulations 4-6) only where needed to improve model convergence and better reflect the observed distribution of zero counts (Figure 3, Table 2):

(3) zi-formula ~ *1*
(4) zi-formula ~ *Natural region*
(5) zi-formula ~ *PC1* + *PC2* + *PC3*
(6) zi-formula ~ (1|*siteID*)

We did not integrate temporal autoregressive structures (van Strien et al., 2004; Korner-Nievergelt et al., 2015) because variograms plotted with the *variog* function of the package *geoR* (v.1.9-3; (Ribeiro Jr & Diggle, 2020) did not reveal issues with temporal autocorrelation. This may result from the difficulty of detecting autocorrelation with just 2-4 observations per site as well as from the six-year gaps between repeated measures (usually accompanied by a change in observer), which may add more variation to model residuals than expected from the remaining temporal pattern.

Table 1 - Overview of model types (main model family, coefficients in the optional zi-binomial model) and number of case study species per model type. Species names are given for the 14 exemplary species shown in this paper. Details for all species are in Appendix 7. Models are ordered according to their parsimony (top = most parsimonious).

model family	binomial model coefficients	# species (%)	exemplary species
pois		3 (4.9%)	European Green Woodpecker (*Picus viridis*), Eurasian Nuthatch (*Sitta europaea*)
nb		13 (21.3%)	Eurasian Blue Tit (*Cyanistes caeruleus*), Common Chiffchaff (*Phylloscopus collybita*)
zip	~ 1	7 (11.5%)	Black Redstart (*Phoenicurus ochruros*), Willow Tit (*Poecile montanus*)
zinb	~ 1	13 (21.3%)	Great Tit (*Parus major*)
zip	~ PCs	3 (4.9%)	Grey Wagtail (*Motacilla cinerea*)
zinb	~ PCs	6 (9.8%)	Eurasian Jay (*Garrulus glandarius*), Common Chaffinch (*Fringilla coelebs*)
zip	~ NR	1 (1.6%)	Common Kestrel (*Falco tinnunculus*)
zinb	~ NR	3 (4.9%)	Barn Swallow (*Hirundo rustica*)
zip	~ (1|ID)	5 (8.2%)	Common Buzzard (*Buteo buteo*)
zinb	~ (1|ID)	7 (11.5%)	Eurasian Magpie (*Pica pica*)

pois = Poisson, nb = negative binomial, zip = zero-inflated Poisson, zinb = zero-inflated negative binomial, PCs = Principal Components PC1 + PC2 + PC3, NR = Natural region, (1|ID) = random intercept of site-ID.

To fit Bayesian models, we used weakly informative prior distributions for coefficients (normal with mean = 0, SD = 2.5 for categorical coefficients, mean = 0, SD = 10 for numeric coefficients) and a maximum tree depth of 10 for the Hamiltonian Monte Carlo algorithm in Stan. Each model ran four Markov chain Monte Carlo chains with 1,000 warm-up and 2,000 post-warm-up samples per chain. We used the 8,000 post-warm-up samples for posterior predictive checks of the model's ability to simulate the observed *abundance* distribution. Criteria included distributional characteristics (mean and standard deviation) as well as the model's ability to reflect extreme values (maximum value) and potential zero inflation (proportion of zero counts, propZ) in the data. In all these cases, we calculated the proportion of simulations exceeding the observed raw data value (Bayesian p-value, Korner-Nievergelt et al. 2015). Bayesian p close to 0.5 imply a good match because the observed values are roughly central within the distribution of simulated data, while values approaching 0 or 1 flag models that clearly under- or overestimated the observed value.

We further checked several conversion indicators of the coefficient estimates: R_{hat}-values ≤ 1.1 (observed max = 1.01) (Brooks & Gelman, 1998), effective posterior samples ≥ 10% of total samples (observed min = 9.4%) and Monte Carlo standard errors ≤ 10% of the standard deviation (observed max = 4.3%) (Korner-Nievergelt et al., 2015). To select the model with the best predictive performance per species, we did a k-fold-cross-validation using 16 folds resulting in a theoretical expected log pointwise predictive density (ELPD) per model, as well as ELPD differences (model with best ELPD compared to others) and the respective standard error of the difference (se ELPD difference) (Bürkner, 2017). When several models resulted in near-identical performance (ELPD difference ± 1.96*se ELPD difference included 0), we continued with the most parsimonious model, i.e., the model with the lowest number of covariates or model components (see Table 1), that fulfilled our conversion indicators. Note that cross-validation leads to a high computational cost: Runtime per model and species without cross-validation span between just one and five minutes, whereas cross-validation (16 additional models) took 15 to 60 minutes per species on a machine with 16 threads.

From the post-warm-up samples we also derived mean covariate coefficient estimates with their 95% credible intervals (CrI) and the posterior probability that the estimate exceeds 0, P(β > 0). Posterior probabilities approaching 0 or 1 indicate increasingly strong evidence for a directional coefficient.

Population trends

Model predictions ± 95% CrI were derived via brms.fitted (Bürkner, 2017) to display trends graphically. When estimating trends over years and differences between natural regions, values of the remaining model covariates were set to their natural region-specific sample mean (continuous covariates), to the level 'none' (for 'observer effect') (Korner-Nievergelt et al., 2015), and group-level effects ('site ID') were generalised beyond the specific grouping level by using the argument re_formula = NA. We derived trends across biogeographic regions by combining these natural region-specific trends according to the natural region's share of the biogeographic region (Atlantic (continental): A = 11.7% (2.1%), B = 20.9% (9.2%), KB = 5.1% (20.1%), KM = 15.1% (0.4%), SB = 0.0% (64.7%), ST = 35.1% (1.2%), metro = 12.1% (2.3%)). Overall trends were derived alike by combining the region-specific trends according to their share of NRW (55.5% Atlantic region and 44.5% continental region). Based on pairwise differences of predicted abundances, we estimated trends as changes in abundance per km² between the start and end date of any desired time period as

$$\text{change} = \frac{N_{ij} - N_{i(j-\Delta t)}}{\Delta t} \quad (7)$$

with N the predicted abundance per km² for the ith posterior draw at times j and $j - \Delta t$, where Δt is the desired time period. If the 95% CrI of these changes in abundance excluded 0, the trend estimate was considered robust. We specifically produced pairwise differences to estimate annual changes (Δt = 1) and a mean long-term trend between 2008 and 2019 (Δt = 12, j = 2019).

Population index

For comparison with other monitoring programmes, we integrated the option to transform predicted mean abundances per km² into an index relative to a user-selected baseline year (here: 2006). Even though the first few years of the monitoring programme suffer from non-representative sampling (see section 'Spatial bias'), weights and smoothing-function enabled accurate estimates in these years without distorting successive estimates (Buckland & Johnston, 2017). Abundance indices were calculated as

$$\text{Abundance index} = \frac{N_{ij}}{\overline{N_j}} \quad (8)$$

with N_{ij} the predicted abundance of the ith posterior draw in year j, and $\overline{N_J}$ the mean predicted abundance of all simulations in the baseline year J (here J = 2006). Based on 10,000 simulations, we calculated the mean index and its 95% CrI for each time step j. Note that this computation calculates an uncertainty also for the baseline year J, which implies that confidence intervals display the uncertainty of the calculated index value and not of the change in index relative to the reference year. Users who prefer a fixed baseline year index without uncertainty need to replace the mean abundance denominator, $\overline{N_J}$ in the formula by N_{iJ} , i.e. the ith simulation in the baseline year.

Data exclusion

Based on an internal validation process of the LANUK, some abundance data were classified as implausible and therefore excluded from the analysis. This process was species-dependent, leading to sample sizes of 608 to 614 per species (full dataset: 614, Appendix 7).

Consistency check

We checked our EAS trends for NRW for consistency with population trends in all West Germany according to the German Common Bird Monitoring scheme (MhB), coordinated by the German association for field ornithologists. MhB study sites are ideally surveyed each year by the same observer (four surveys per site between 10 March and 20 June; full programme details in Kamp et al. (2021)).

The consistency analysis included 59 widely distributed species spanning a broad range of habitat associations and breeding strategies for which we had trend estimates available from the MhB and from the EAS. It is obviously difficult to compare trend estimates between programmes that rest on different methodologies and survey efforts (nine vs. four surveys per year), have different spatial coverage (NRW vs. West Germany) with just a partial match in study sites, and employ fundamentally different analytical approaches (GAMM smoothers in EAS vs. yearly point estimates in MhB). Nevertheless, largely consistent estimates from EAS and MhB would reassure that the analytical approach developed for rolling sampling strategies produces reliable trends that are robust to the underlying survey design. With these limitations in mind, we expected that yearly samples in the MhB versus 6-yearly samples in the EAS should generate largely consistent long-term trend estimates, except for cases where a species' biology would objectively favour one survey and analysis routine over the other (see Discussion).

To assess trend consistency we calculated two parameters for each species: (i) a Pearson 'correlation' coefficient between the annual TRIM-based MhB indices and the annual EAS-indices extracted from model smoothers between 2005 and 2020, and (ii) the Median Symmetric Accuracy (Morley et al., 2018), which estimates the median percentage error between both annual indices I_j:

(9) $$\text{Median Symmetric Accuracy} = 100 * \exp\left(median\left(abs\left(\log\left(\frac{I_{MhBj}}{I_{EASj}}\right)\right)\right)\right) - 1$$

Note that the baseline year 2006 (both indices = 1) was excluded for both methods.

Results

Breeding bird trends were analysed for 61 out of 148 bird species (full detail in Appendix 6, 7), but we focus the description of model assessment results on 14 exemplary species (Table 1). Exemplified data for four species, script, and code are available from Github (https://github.com/m-rieger/EAS_bird; Rieger et al., 2025a) as well as a package with helper functions (https://github.com/m-rieger/EAS; Rieger, 2024).

Distribution characteristics: Species-specific optimisation

Model selection via k-fold cross validation resulted in different best-performing model families and a species-specific selection of coefficients added to the binomial part of zero-inflated models (Table 1, species-specific overview in Appendix 7). We illustrate below the selection of model structure on four species that strongly vary in overall mean abundance, abundance dispersion, and the proportion of sites with zero counts: European Green Woodpecker, Eurasian Blue Tit, Black Redstart, and Eurasian Jay. The four measures that inform abundance distribution (propZ, mean, SD, max) can – but do not necessarily need to – vary with each other, so that an over- or underestimation of zero counts often goes along with an under- or overestimation of the population mean, and an over- or underestimation of SD with an over- or underestimation of maximum abundance.

Table 2 - Examples for model assessment and procedure to select species-specific models from six alternative model structures (for further species and models see Appendix 3). Models differ in family and the presence of a zero-inflated model component (zinb and zip), the latter also in binomial model coefficients. Model assessment quantifies whether simulated data from the model is consistent with the observed response variable (abundance) with respect to its proportion of zeros (propZ), mean and maximum value, and standard deviation (SD). Bayesian p-values close to 0.5 indicate that the observed values are central within the posterior distribution of simulated raw datasets (8000 in total), indicating good model fit. Values close to 0 and 1 indicate substantial under- or overestimation and thus poor model fit. Final model selection is based on ELPD differences by selecting the most parsimonious model (bold, top to bottom) out of all models with an ELPD difference ± 1.96*SE of ELPD difference including 0 (bold values). Abbreviations see Table 1.

species	model family	binomial model coefficients	Bayesian p-value				ELPD	
			propZ	mean	SD	max	diff.	se diff.
European Green Woodpecker *Picus viridis*	**pois**		0.01	0.49	0.79	0.65	**-11.86**	**7.89**
	nb		0.01	0.42	0.62	0.68	-204.94	47.02
	zip	~ 1	0.12	0.44	0.87	0.72	**-6.65**	**6.77**
	zinb	~ 1	0.13	0.46	0.91	0.80	**-8.06**	**6.73**
	zip	~ PCs	0.16	0.46	0.88	0.71	**-3.66**	**6.92**
	zinb	~ PCs	0.16	0.48	0.90	0.76	-18.57	7.91
Eurasian Blue Tit *Cyanistes caeruleus*	pois		0	0.50	0.01	0.02	-510.17	69.13
	nb		0	0.64	0.70	0.37	**-11.2**	**5.77**
	zip	~ 1	0.10	0.34	0.01	0.02	-498.39	66.54
	zinb	~ 1	0.07	0.58	0.69	0.37	-19.9	8.09
	zip	~ PCs	0.11	0.39	0.01	0.02	-509.75	71.86
	zinb	~ PCs	0.07	0.60	0.70	0.38	**-6.2**	**5.83**
Black Redstart *Phoenicurus ochruros*	pois		0	0.51	0.56	0.47	-23.37	10.14
	nb		0	0.59	0.82	0.59	-3654.6	780.81
	zip	**~ 1**	0	0.30	0.48	0.45	**-8.51**	**9.42**
	zinb	~ 1	0	0.42	0.76	0.56	**-4.01**	**7.52**
	zip	~ PCs	0	0.42	0.54	0.48	**-12.87**	**9.19**
	zinb	~ PCs	0	0.51	0.79	0.51	**0**	**0**
Eurasian Jay *Garullus glandarius*	pois		0	0.50	0.76	0.77	-37.68	11.47
	nb		0	0.69	0.89	0.70	-117.44	22.38
	zip	~ 1	0	0.31	0.78	0.76	-27.5	8.37
	zinb	~ 1	0	0.34	0.83	0.81	-28.52	8.11
	zip	~ PCs	0.19	0.36	0.77	0.67	-23.57	10.83
	zinb	**~ PCs**	0.19	0.39	0.81	0.72	**-15.08**	**10.25**

European Green Woodpecker (Table 2, Figure 3a) represents species with typically low territory numbers and many zero counts. While all models underestimated the number of zero counts, a Poisson model sufficiently captured other distribution parameters, resulting in a good predictive performance.

Eurasian Blue Tit (Table 2, Figure 3b) is an abundant and widespread species that occurs in nearly all study sites. Here, abundance varied clearly more within sites and/or between year than

reflected by a Poisson distribution. This issue of an underestimated SD was solved by using a negative binomial model family, even though leading to a slight overestimated SD.

Black Redstart (Table 2, Figure 3c) is widespread at typically medium densities, resulting in a larger fraction of unoccupied sites than expected under a Poisson distribution. All models failed to capture this zero-bias, but models with a zero-inflation component were closer to the observed value. Since zero-inflated models mostly resulted in comparable ELPDs, we used the most parsimonious model (zero-inflated Poisson with no additional binomial coefficient) for further analyses.

Eurasian Jay (Table 2, Figure 3d) is a widespread species with low territory numbers. Using zero-inflated models with environmental PCs as binomial model coefficient sufficiently captured the observed number of zero counts, and the zero-inflated negative binomial model resulted in the best predictive performance.

Spatial bias

For many species, (long-term) trends varied between natural regions, confirming the need to account for spatial bias. Especially long-term trends in metropolitan areas differed considerably from trends in other natural regions, usually showing steeper decreases in abundance per km² (except for a steeper increase in Black Redstart, Figure 4). Ignoring the overrepresentation of metropolitan sites (or any other unbalance in natural region samples) in the EAS dataset would therefore result in biased (long-term) trends for biogeographic regions and overall. In case of Eurasian Magpie and Eurasian Nuthatch, trends would be more negative and for Black Redstart more positive.

Observer effects

We found a strikingly inhomogeneous distribution of observer effects across years, bearing substantial potential for biased population trend estimates when unaccounted for. High total abundances occurred disproportionally often since 2015, and strikingly low abundances before 2006 (Figure 5, left), irrespective of the chosen threshold value (Appendix 4). Models ignoring observer effects generally produced more positive long-term trend estimates, i.e., resulted in steeper increases or less steep declines than models with the covariate *Observer* (Figure 5, right). For Chaffinch, correcting for observer effects even reversed the increase in abundance in the non-corrected model to a decrease in the corrected model (Figure 5, right). OE-corrected trend estimates were generally more consistent with West German trend estimates from the MhB programme (Appendix 4) where consecutive surveys at a given site are always from the same observer.

Consistency check

Correlation coefficients between our annual EAS indices and West German MhB indices revealed solid matches – i.e., with correlation coefficients and their 95% CI > 0 – for 34 out of 59 species (e.g., Nuthatch and Chiffchaff in Figure 6a, b). Only five species (e.g., Eurasian Jay in Figure 6d) tended to have negatively correlated yearly indices, but their 95% CI always included 0. Likewise, median symmetric accuracies (MSA) between index estimates were reasonably low, with 43 (or 26) out of 59 species deviating ≤ 20% (or ≤ 10%). Strong positive correlations do not necessarily go along with low MSA values, because the latter are rather sensitive to the chosen index baseline year as illustrated by the Chiffchaff data (Figure 6b). Here, EAS- and MhB-analyses revealed rather consistent trend patterns for the period 2007–2020. Yet, the MSA-values were high, first because the exceptionally low MhB index in the baseline year 2006 shifted most other annual MhB-index values up so they exceeded the EAS values, but also because the smoothed trend did not reflect the magnitude of index differences between the early years 2005 + 2006 and later years. In contrast, Great Tit and Eurasian Jay exemplify how poor correlation between annual index values can go along with low MSA values (Figure 6c, d), here because a rather stable vs. more fluctuating trend (Great Tit) that is identified by a weak correlation shows only minor

deviations in trends (low MSA) or largely overlapping but slightly diverging trends (Eurasian Jay, especially due to year 2005) fail to correlate. Correlation coefficients, MSA values, and trend displays for all 59 species are in Appendix 5.

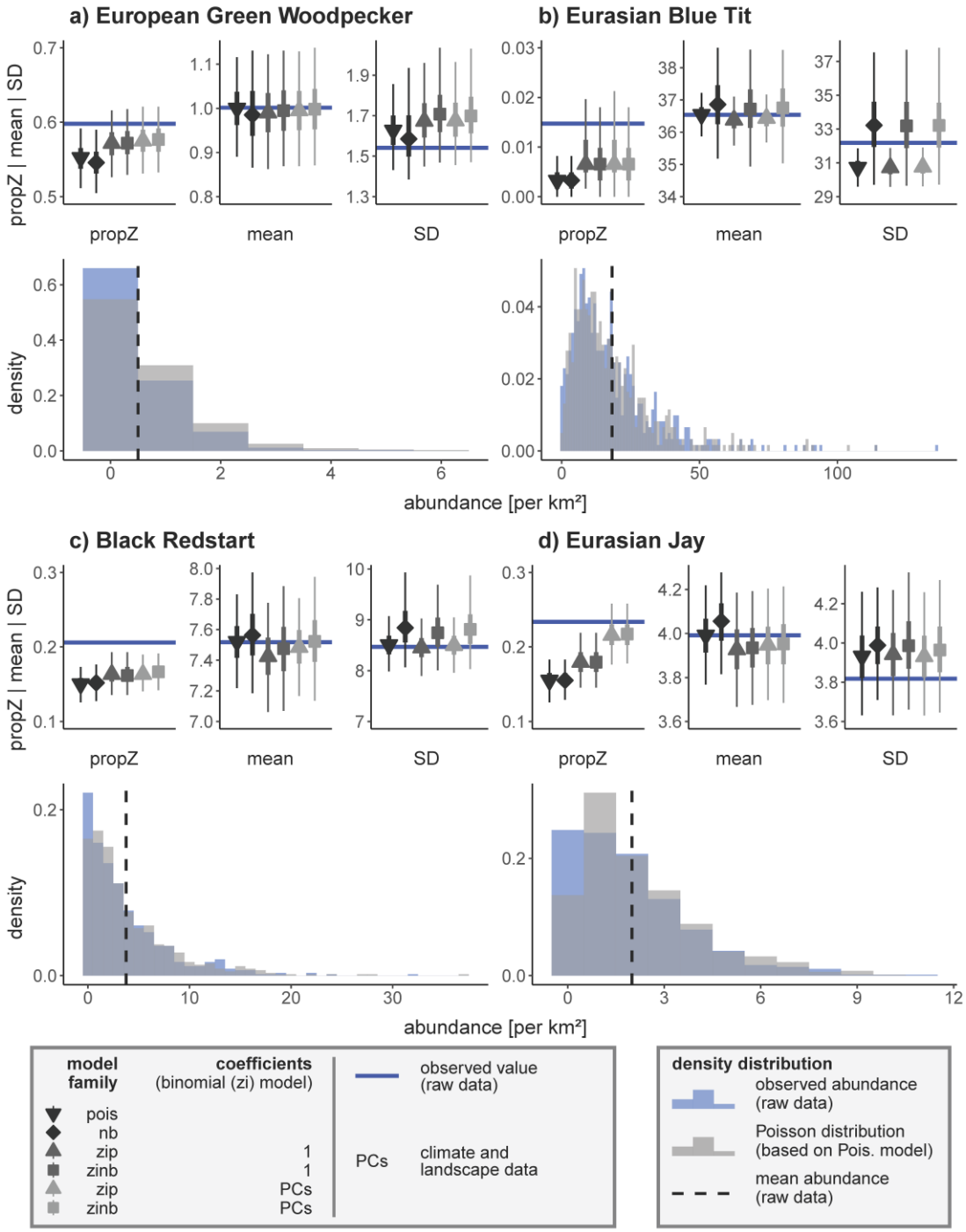

Figure 3 - Reasoning for selecting appropriate model structures for four species. Upper panels: Model performance with respect to the proportion of zero counts (propZ), mean, and standard deviation (SD) of the response variable 'abundance'. Symbols with error bars display the median ± 50% CrI (thick bars) and 95% CrI (thin bars) for 8000 posterior raw datasets simulated from the selected models as given in the legend. Optimal models have a close match between observed and model-predicted data. Lower panels: Density distributions of observed abundances (blue, dashed line = mean) and Poisson distributions (grey) based on simulated responses derived from the respective Poisson model. Y-axes differ in scale.

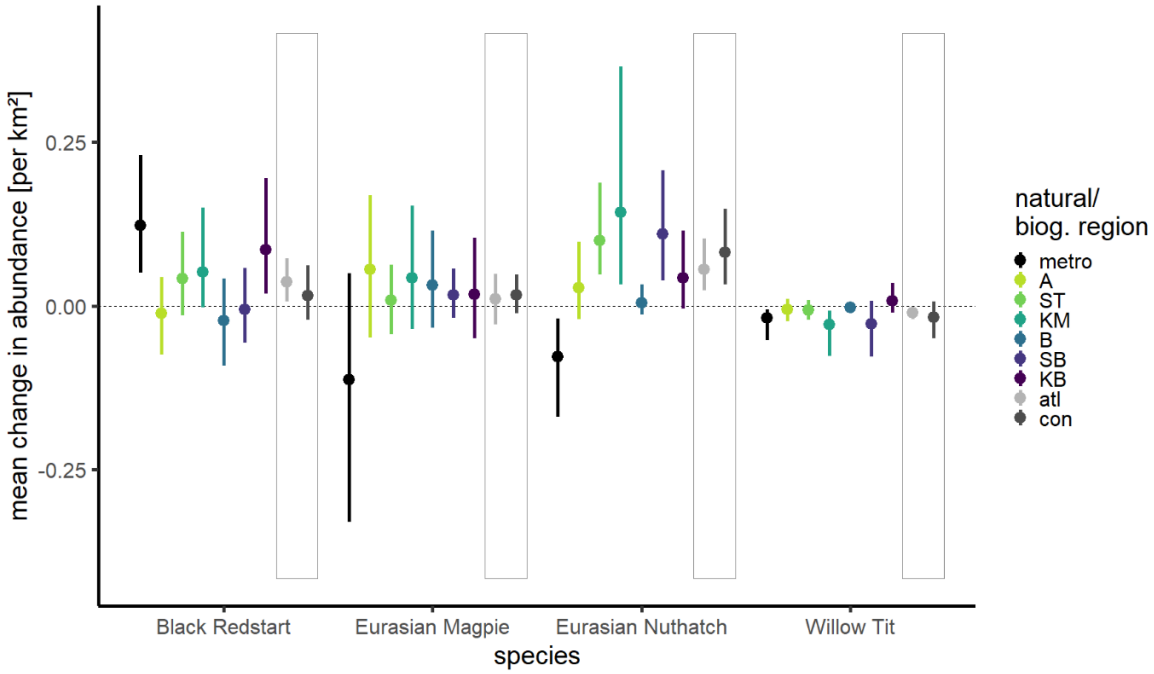

Figure 4 - Mean annual change in abundance per km² (long-term period 2008-2019) per natural region (See Figure 1 for acronyms) and combined per overarching biogeographic region (atlantic - atl, and continental - con, grey boxes) for four example species.

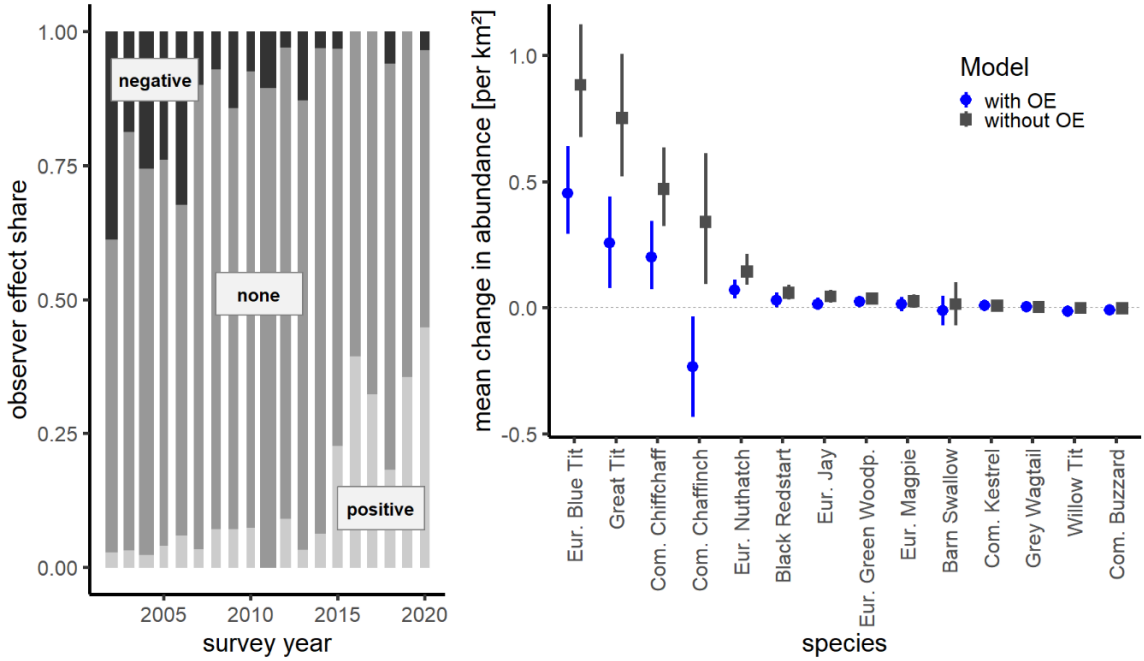

Figure 5 - Left: Proportion of surveyed EAS sites per observer effect level per year. Bar widths are proportional to the number of surveyed sites per year. Right: Mean annual change in abundance per km² (long-term period 2008-2019) estimated from models with and without the covariate observer effects for 14 species (example trend curves in Appendix 4).

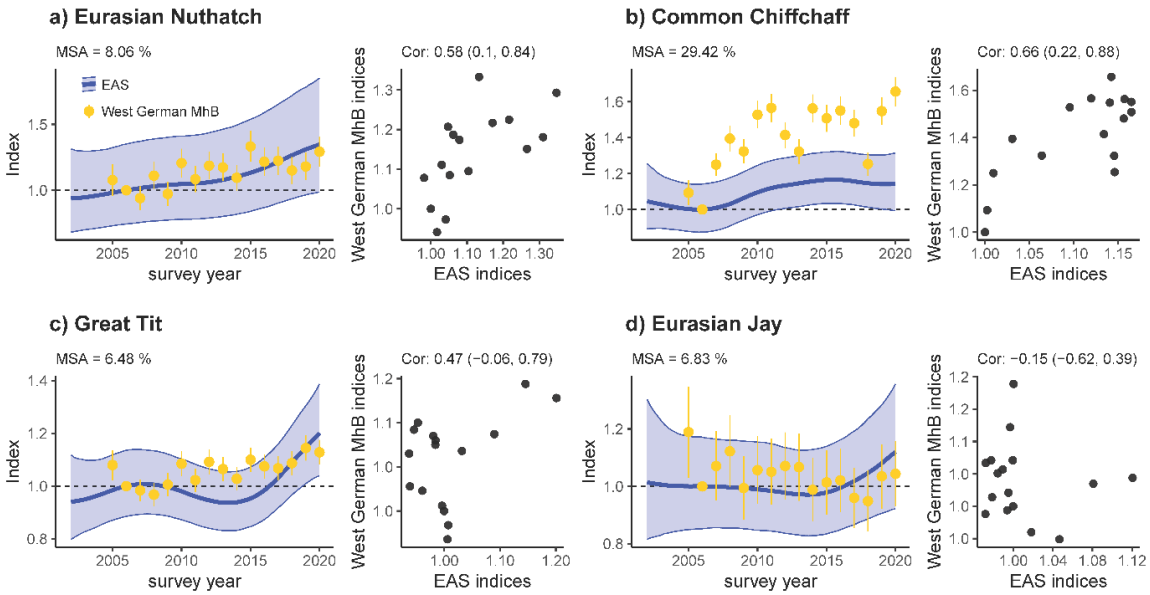

Figure 6 - Trend comparison of EAS monitoring programme (this study, confidence intervals CI show uncertainty in the estimated index) and West German data from the German Common Bird Monitoring scheme (MhB, for comparison, CIs show uncertainty in index change) for four species. Left (per panel): Median Symmetric Accuracy (MSA) based on annual comparisons of indices. Right (per panel): correlation and correlation coefficients (± 95% CI) of annual indices from 2005 to 2020. Both approaches exclude the baseline year 2006.

Discussion

Count data are the raw unit for many population trend analyses, but their distribution poses several challenges during statistical analyses to account for overdispersion (42 out of 61 species in our current dataset) and/or zero inflation (45 out of 61 species). Moreover, many biodiversity monitoring programmes rest on ‘rolling’ sampling designs where each study site is visited only every so many years and observer identity frequently changes between years. We developed a workflow that takes these challenges into account (Figure 7) (Rieger, 2024; Rieger et al., 2025a). First, we derive a routine that allows informed decisions about the most appropriate combination of residual families (Poisson or negative binomial), model covariates (e.g., habitat characteristics), and zero-inflation formulations to reflect species-specific data distributions. Second, we develop a correction factor that buffers population trend estimates for variation in observer expertise. Third, we integrate region-specific trends that adjust for between-year variation in the representation of habitat or natural regions within the yearly subset of sampled sites. Finally, by using generalised additive mixed models, we account for missing values due to rolling surveys. With these corrections in place, we find – within limits of the comparison – good consistency between the EAS trends and trends from the standard German Common Bird Monitoring scheme.

Distribution characteristics: Species specific optimisation

We found substantial variation in model structures that best reflected the empirical abundance distributions and fraction of structural zeros across the 61 study species. Model formulations spanned from simple Poisson or negative binomial models (e.g., European Green Woodpecker, Eurasian Blue Tit; 26.2 % of all modelled species) to models with elaborate zero inflation formulae to account for variation in the fraction of structural zeros across natural regions, study sites, or environmental covariates (e.g., Great Spotted Woodpecker or Willow Tit; 73.8 % of all modelled species, Table 1). This variation often tied in with breeding ecologies (cf. examples in section ‘Distribution characteristics: Species-specific optimisation’). Widespread and abundant species

with intermediate territory counts in many study sites typically required rather simple count models but no correction for structural zeroes. In contrast, heterogeneously distributed species with a high fraction of unoccupied sites or colonial breeders with often large territory numbers at the few occupied sites almost exclusively required the integration of zero inflation formulae, possibly connected with controls for variation in zero frequencies between regions, sites or environments. This diversity in distribution and abundance patterns is typical for most (bird) monitoring programmes independent of the chosen modelling approach, with similar choices documented elsewhere (Etterson et al., 2009; Tirozzi et al., 2021, 2022; Hernández-Navarro et al., 2023).

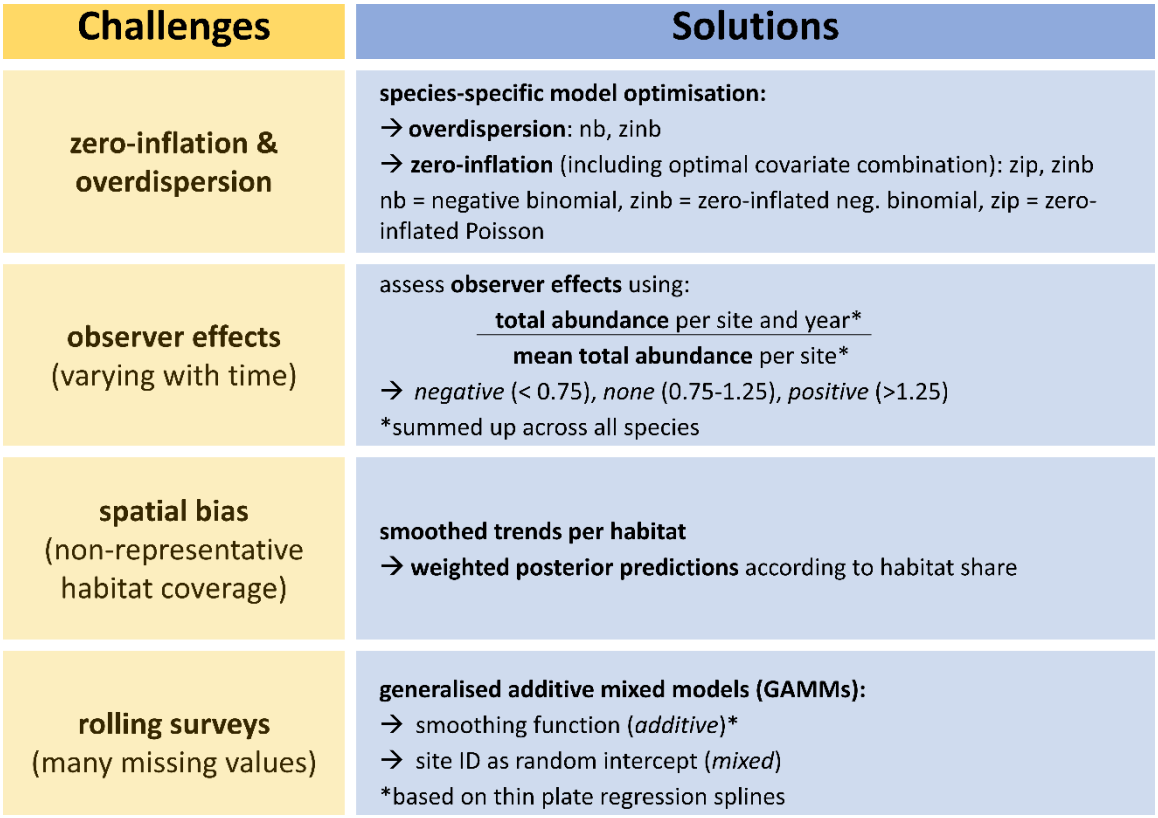

Figure 7 - Workflow to address several challenges that arise when analysing breeding bird trends.

Spatial bias

Modelling trends per natural region is a useful tool to reduce distorted trends due to spatial bias. This was exemplified by species such as Black Redstart, Eurasian Magpie, and Eurasian Nuthatch, showing striking diverging trends between metropolitan areas and other natural regions (Figures 2, 4), which would otherwise bias regional or overall trends if discrepancies between natural region shares would be ignored. Similar distortions of trends or species distributions due to spatial bias often occur when using citizen science data since the sampled sites are selected by the observer and thus biased by its preferences (e.g., urban sites, sites of ecological interest (Johnston et al., 2020; Bowler et al., 2022))

Monitoring schemes should obviously aim to avoid the extreme disbalance in sampling that characterises the early phase of the EAS monitoring, where each year focused on a subset of natural regions. Such bias is difficult to correct *a posteriori* and bears the risk that compensating for missing values leads to a high level of uncertainty, masking possible trends. However, when the yearly sampling subsets are representative and include all present natural regions, as in the EAS programme since 2013 (Figure 2), our approach can unfold its full capacity by accounting for minor bias in habitat coverage or the overrepresentation of metropolitan areas among study sites.

Observer effects

We found negative observer effects to occur disproportionally often during the early years of the EAS programme but positive effects primarily in recent years. This likely arises from a combination of a temporal increase in expertise with ongoing involvement in the EAS programme but also the new involvement of observers with individually higher population estimates during the later programme years, with both effects visible in Figure 4.3 of Appendix 4. This unfavourable combination of observer effects apparently caused substantial deviations in our abundance estimates compared to West German breeding bird trends, with a systematic shift towards more positive trends compared to MhB trends. In many cases, this bias was successfully mitigated by adding observer effect as a model covariate, now yielding trend estimates that were far more consistent with those of the West German Common Bird Monitoring programme (MhB, Appendix 4).

Our approach to categorise observer effects from site-specific abundance data risks to mask drastic increases or declines in true bird abundance, e.g., after a substantial change in habitat quality or land-use. Such extreme shifts, however, will typically have diverging species-specific effects on abundance with winners and losers (Lemoine et al., 2007), and thus will massively affect total abundance across species just in exceptional extreme cases. Moreover, steady increases or declines in total abundance with habitat quality will also change mean total abundance across survey years, so that the threshold beyond which survey years are flagged as ’extreme‘ (positive or negative) also increases or decreases accordingly. Our categorisation fails, however, to identify cases of species-specific observer effects, such as insufficient expertise in discriminating ‘difficult’ species (e.g., songs of Garden Warbler vs. Blackcap) since total abundance is not affected by this, or hearing impairment for high pitched vocalisations (e.g., Goldcrest and Firecrest). For EAS, such cases are marked as implausible via an internal validating process and excluded from analysis (see section ‘Data exclusion’).

Alternative indices may capture components of observer effort beyond our rather simplistic representation of expertise. A widespread approach integrates survey duration or transect length as model covariates, or combines both measures into survey duration per unit length (Kéry et al., 2005). Kéry et al. (2005) found higher survey effort to increase the detection rates of many bird species, resulting in higher abundance estimates. Others integrated observer age as a (quadratic) model covariate to correct for age-related changes in survey completeness (Farmer et al., 2014). Citizen Science data, e.g. those reported through online platforms such as ornitho (https://www.ornitho.de/) or ebird (https://ebird.org/), further allow estimating observer- and species-specific detection rates from species checklists, providing even more precise correction factors (Johnston et al., 2018). So far, the EAS monitoring programme cannot provide the data required to extract any of these covariates (i.e., effort, age, detection rates), but we highly recommend their integration to more precisely correct for possible observer effects in the future.

Some of the observer effects inherent to the EAS dataset likely arise from individual differences in the approach to delineate breeding territories. In future refinements of the program, this could be mitigated by using point observations per survey instead of territories as the basis for trend analyses, possibly in hierarchical models comparable to those used in other monitoring programmes such as the Swiss Breeding Bird survey (Kéry et al., 2005; Strebel et al., 2020). Alternatively, territory delineation could be automated from raw point observations, e.g., using the AutoTerri algorithm from TerriMap online developed by the Swiss Ornithological Institute (Wechsler, 2018).

Consistency check

Population trend estimates for 59 species revealed a reasonably close match between the GAMM-based trend smoothers applied on the EAS dataset and TRIM-based yearly point estimates applied in the West German Common Bird Monitoring scheme. Despite substantial differences in the chosen modelling approach and spatial coverage, most trend estimates had solid positive correlations and/or a good Median Symmetric Accuracy between annual indices (Figure 6,

Appendix 5). In many cases, smoothed GAMM-trends for the EAS data captured even short-term population fluctuations at a 3–7-year scale, similar to the – by definition – more fine-grained yearly MhB indices (e.g., Common Blackbird, Eurasian Wren, Firecrest, Appendix 5). Neutral or even negative correlations between yearly EAS- and MhB-indices occurred primarily in two species subsets. The first concerns colonial birds (e.g., Common Swift, Eurasian Tree Sparrow, Common House Martin, Barn Swallow, Appendix 5) where trend estimates are highly sensitive to the share of study sites with colonies present, the influence of few large colonies on the trend estimates, the precision of nest counts, and observer access to a given colony (Südbeck et al., 2005; LANUV, 2016a). The second subset concerns species with pronounced affinity to urban areas as derived from low or high coefficient estimates for the linear effect of PC3 (Appendix 6), where affinity can be positive (e.g., Eurasian Magpie, Dunnock, Common House Martin, Common Kestrel and Black Redstart) or negative (e.g., Common Chaffinch, Eurasian Jay, Marsh Tit or Crested Tit). Given an exceptionally high share and density of urban areas in NRW compared to other West German federal states, NRW trends are plausibly more positive than West German MhB trends for urban specialists (e.g., Eurasian Magpie, Dunnock, Common Kestrel, Black Redstart, Appendix 5) and more negative for non-urban species (e.g. Common Chaffinch and Crested Tit, Appendix 5).

Conclusion

We developed a modelling routine for bird population trend analyses that can handle several common problems in monitoring data. Our approach accounts for unbalanced sampling of natural regions, optimises species-specific model structure with respect to zero-inflation and overdispersion, partially accounts for variation in observer expertise, and integrates GAMM-based smoothing to bridge even extensive gaps between replicated surveys in a ‘rolling’ sampling design. Our consistency check against trends from the Germany Common Bird Monitoring programme indicates that our routine produces reliable and robust trends for most species. The R script and package provided with this study can be adapted to other monitoring programmes with comparable survey designs and data structures.

Acknowledgements

We thank the many observers for contributing to the EAS and MhB monitoring programmes, Matteo Santon for statistical and computational advice, and Jakob Katzenberger, Johannes Kamp, and Johannes Wahl for comments on earlier versions of this workflow. We also thank Matthieu Paquet and two anonymous referees for their helpful feedback during the submission process. Preprint version 3 of this article has been peer-reviewed and recommended by Peer Community In Ecology (https://doi.org/10.24072/pci.ecology.100748; Paquet, 2025).

Funding

The development of this workflow has been financially supported by State Agency for Nature, Environment and Climate in North Rhine-Westphalia (LANUK, former LANUV) to University of Tübingen.

Conflict of interest disclosure

The authors declare that they comply with the PCI rule of having no financial conflicts of interest in relation to the content of the article.

Data, scripts, code and supplementary information availability

A data example for four species, R script, and code are available from Zenodo (https://doi.org/10.5281/zenodo.12518872; Rieger et al., 2025a) as well as an Appendix containing

further figures, model outputs and detailed descriptions (https://doi.org/10.5281/zenodo.15267093; Rieger et al., 2025b), and a package with helper functions (https://doi.org/10.5281/zenodo.12517388; Rieger, 2024).

References

ATKIS. (2013). Amtliches Topographisch-Kartographisches Informationssystem. Retrieved from https://www.adv-online.de/AdV-Produkte/Geotopographie/ATKIS/

Blasco-Moreno A, Pérez-Casany M, Puig P, Morante M, Castells E (2019) What does a zero mean? Understanding false, random and structural zeros in ecology. *Methods in Ecology and Evolution,* **10**, 949-959. https://doi.org/10.1111/2041-210X.13185

Bogaart P, van der Loo M, Pannekoek J (2020) Package 'rtrim' - Trends and Indices for Monitoring Data, version 2.1.1. *R package*. https://doi.org/10.32614/CRAN.package.rtrim

Bowler DE, Callaghan CT, Bhandari N, Henle K, Benjamin Barth M, Koppitz C, Klenke R, Winter M, Jansen F, Bruelheide H (2022) Temporal trends in the spatial bias of species occurrence records. *Ecography,* **2022**, e06219. https://doi.org/10.1111/ecog.06219

Brooks SP, Gelman A (1998) General methods for monitoring convergence of iterative simulations. *Journal of computational and graphical statistics,* **7**, 434-455. https://doi.org/10.1080/10618600.1998.10474787

Buckland S, Johnston A (2017) Monitoring the biodiversity of regions: Key principles and possible pitfalls. *Biological Conservation,* **214**, 23-34. https://doi.org/10.1016/j.biocon.2017.07.034

Bürkner P-C (2017) brms: An R package for Bayesian multilevel models using Stan. *Journal of statistical software,* **80**, 1-28. https://doi.org/10.18637/jss.v080.i01

Burns F, Eaton MA, Burfield IJ, Klvaňová A, Šilarová E, Staneva A, Gregory RD (2021) Abundance decline in the avifauna of the European Union reveals cross-continental similarities in biodiversity change. *Ecology and Evolution,* **11**, 16647-16660. https://doi.org/10.1002/ece3.8282

Campbell H (2021) The consequences of checking for zero-inflation and overdispersion in the analysis of count data. *Methods in Ecology and Evolution,* **12**, 665-680. https://doi.org/10.1111/2041-210X.13559

CDC. (2010). Deutscher Wetterdienst Climate Data Center: Vieljährige Stationsmittelwerte für die Klimareferenzperiode 1981-2010. Retrieved from https://www.dwd.de/DE/klimaumwelt/cdc/cdc_node.html

Dakki M, Robin G, Suet M, Qninba A, El Agbani MA, Ouassou A, El Hamoumi R, Azafzaf H, Rebah S, Feltrup-Azafzaf C (2021) Imputation of incomplete large-scale monitoring count data via penalized estimation. *Methods in Ecology and Evolution,* **12**, 1031-1039. https://doi.org/10.1111/2041-210X.13594

Etterson MA, Niemi GJ, Danz NP (2009) Estimating the effects of detection heterogeneity and overdispersion on trends estimated from avian point counts. *Ecological Applications,* **19**, 2049-2066. https://doi.org/10.1890/08-1317.1

Farmer RG, Leonard ML, Mills Flemming JE, Anderson SC (2014) Observer aging and long-term avian survey data quality. *Ecology and Evolution,* **4**, 2563-2576. https://doi.org/10.1002/ece3.1101

Fewster RM, Buckland ST, Siriwardena GM, Baillie SR, Wilson JD (2000) Analysis of population trends for farmland birds using generalized additive models. *Ecology,* **81**, 1970-1984. https://doi.org/10.1890/0012-9658(2000)081[1970:AOPTFF]2.0.CO;2

Gabry J, Češnovar R (2020) Cmdstanr: R interface to 'CmdStan'.

Hernández-Navarro AJ, Robledano F, Jiménez-Franco MV, Royle JA, Calvo JF (2023) Long-term trends of local bird populations based on monitoring schemes: are they suitable for justifying management measures? *Journal of Ornithology*, 1-13. https://doi.org/10.1007/s10336-023-02114-3

Jennings K. (2021). *Deploying data for nature conservation: How monitoring data is used to inform conservation policy and practice [Keynote address]*. Paper presented at the BOUsci21 - Developments in monitoring science, United Kingdom, November 24-25.

Jiguet F (2009) Method learning caused a first-time observer effect in a newly started breeding bird survey. *Bird Study,* **56**, 253-258. https://doi.org/10.1080/00063650902791991

Jiguet F, Barbet-Massin M, Devictor V, Jonzén N, Lindström Å (2013) Current population trends mirror forecasted changes in climatic suitability for Swedish breeding birds. *Bird Study,* **60**, 60-66. https://doi.org/10.1080/00063657.2012.733337

Johnston A, Fink D, Hochachka WM, Kelling S (2018) Estimates of observer expertise improve species distributions from citizen science data. *Methods in Ecology and Evolution,* **9**, 88-97. https://doi.org/10.1111/2041-210X.12838

Johnston A, Fink D, Reynolds MD, Hochachka WM, Sullivan BL, Bruns NE, Hallstein E, Merrifield MS, Matsumoto S, Kelling S (2015) Abundance models improve spatial and temporal prioritization of conservation resources. *Ecological Applications,* **25**, 1749-1756. https://doi.org/10.1890/14-1826.1

Johnston A, Moran N, Musgrove A, Fink D, Baillie SR (2020) Estimating species distributions from spatially biased citizen science data. *Ecological Modelling,* **422**, 108927. https://doi.org/10.1016/j.ecolmodel.2019.108927

Kamp J, Frank C, Trautmann S, Busch M, Dröschmeister R, Flade M, Gerlach B, Karthäuser J, Kunz F, Mitschke A (2021) Population trends of common breeding birds in Germany 1990–2018. *Journal of Ornithology,* **162**, 1-15. https://doi.org/10.1007/s10336-020-01830-4

Kéry M, Royle JA, Schmid H (2005) Modeling avian abundance from replicated counts using binomial mixture models. *Ecological Applications,* **15**, 1450-1461. https://doi.org/10.1890/04-1120

Klvaňová A, Voříšek P, Gregory RD, van Strien A, Gmelig Meyling A (2009) Wild birds as indicators in Europe: latest results from the Pan-European Common Bird Monitoring Scheme (PECBMS). *Avocetta,* **33**, 7-12

Knape J (2016) Decomposing trends in Swedish bird populations using generalized additive mixed models. *Journal of Applied Ecology,* **53**, 1852-1861. https://doi.org/10.1111/1365-2664.12720

König H (2020) Standards und Indikatorartengruppen - Erfahrungen aus der ÖFS in Nordrhein-Westfalen. In: *Umfassendes bundesweites Biodiversitätsmonitoring* eds Züghart W, Stenzel S, & Fritsche B) (Vol. 585), pp. 17-32. BfN Schriften.

Korner-Nievergelt F, Roth T, Von Felten S, Guélat J, Almasi B, Korner-Nievergelt P (2015) *Bayesian data analysis in ecology using linear models with R, BUGS, and Stan*. Academic Press. https://doi.org/10.1016/b978-0-12-801370-0.00004-6

LANUV (2016a) Arbeitsanleitung für Brutvogel-Revierkartierungen im Auftrag des LANUV NRW. *Landesamt für Natur, Umwelt und Verbraucherschutz Nordrhein-Westfalen, Recklinghausen, Germany*, 1-79

LANUV (2016b) Daten zur Natur in Nordrhein-Westfalen 2016 - LANUV-Fachbericht 83. *Landesamt für Natur, Umwelt und Verbraucherschutz Nordrhein-Westfalen, Recklinghausen, Germany*, 1-216

Lemoine N, Bauer H-G, Peintinger M, Böhning-Gaese K (2007) Effects of climate and land-use change on species abundance in a central European bird community. *Conservation Biology,* **21**, 495-503. https://doi.org/10.1111/j.1523-1739.2006.00633.x

Link WA, Sauer JR (1998) Estimating population change from count data: application to the North American Breeding Bird Survey. *Ecological Applications,* **8**, 258-268. https://doi.org/10.1890/1051-0761(1998)008[0258:EPCFCD]2.0.CO;2

Morley SK, Brito TV, Welling DT (2018) Measures of model performance based on the log accuracy ratio. *Space Weather,* **16**, 69-88. https://doi.org/10.1002/2017SW001669

Niemelä J (2000) *Biodiversity monitoring for decision-making.* In: Annales Zoologici Fennici: pp. 307-317, JSTOR.

Pannekoek J, van Strien AJ (2001) TRIM 3 manual (Trends & Indices for Monitoring Data). *CBS Statistics Netherlands, Voorburg, The Netherlands.*

Paquet M (2025) Discarding data or dealing with bias? *Peer Community in Ecology,* **100748**. https://doi.org/10.24072/pci.ecology.100748

Pöysä H, Rintala J, Lehikoinen A, Väisänen RA (2013) The importance of hunting pressure, habitat preference and life history for population trends of breeding waterbirds in Finland. *European Journal of Wildlife Research,* **59**, 245-256. https://doi.org/10.1007/s10344-012-0673-8

R Core Team (2024) R: a language and environment for statistical computing. *R Foundation for Statistical Computing website*

Ribeiro Jr PJ, Diggle PJ (2020) Package 'geoR' - Analysis of Geostatistical Data. *R package*. https://doi.org/10.32614/CRAN.package.geoR

Rieger MR (2024) EAS - Module to analyse population trends from monitoring data with highly structured sampling designs. *Zenodo*. https://doi.org/10.5281/zenodo.12517388

Rieger MR, Grüneberg C, Oberhaus M, Trautmann S, Parepa M, Anthes N (2025a) EAS_bird - Data and script of 'Bird population trend analyses for a monitoring scheme with a highly structured sampling design'. *Zenodo*. https://doi.org/10.5281/zenodo.12518872

Rieger MR, Grüneberg C, Oberhaus M, Trautmann S, Parepa M, Anthes N (2025b) Supplement to 'Bird population trend analyses for a monitoring scheme with a highly structured sampling design'. *Zenodo*. https://doi.org/10.5281/zenodo.15267093

Sauer JR, Pardieck KL, Ziolkowski Jr DJ, Smith AC, Hudson M-AR, Rodriguez V, Berlanga H, Niven DK, Link WA (2017) The first 50 years of the North American breeding bird survey. *The Condor: Ornithological Applications,* **119**, 576-593. https://doi.org/10.1650/CONDOR-17-83.1

Sauer JR, Peterjohn BG, Link WA (1994) Observer differences in the North American breeding bird survey. *The Auk,* **111**, 50-62. https://doi.org/10.2307/4088504

Strebel N, Dröschmeister R, Schmid H, Stützle I, Trautmann S, Wahl J (2020) Ein Vergleich zwischen revier-und individuenbasierten Verfahren zum Abschätzen von Brutbestandsindizes im Monitoring häufiger Brutvögel. *Die Vogelwelt,* **140**, 183-206

Südbeck P, Andretzke H, Gedeon K, Schikore T, Schröder K, Fischer S, Sudfeldt C (2005) *Methodenstandards zur Erfassung der Brutvögel Deutschlands*. Max-Planck-Institut für Ornithologie. Vogelwarte Radolfzell.

Tirozzi P, Orioli V, Dondina O, Kataoka L, Bani L (2021) Species Traits Drive Long-Term Population Trends of Common Breeding Birds in Northern Italy. *Animals,* **11**, 3426. https://doi.org/10.3390/ani11123426

Tirozzi P, Orioli V, Dondina O, Kataoka L, Bani L (2022) Population trends from count data: handling environmental bias, overdispersion and excess of zeroes. *Ecological Informatics,* **69**, 101629. https://doi.org/10.1016/j.ecoinf.2022.101629

van Strien AJ, Pannekoek J, Gibbons DW (2001) Indexing European bird population trends using results of national monitoring schemes: a trial of a new method. *Bird Study,* **48**, 200-213. https://doi.org/10.1080/00063650109461219

van Strien AJ, Pannekoek J, Hagemeijer W, Verstrael T (2004) A loglinear Poisson regression method to analyse bird monitoring data. *Bird Census News,* **13**, 33-39

Vorisek P, Gregory RD, Van Strien AJ, Meyling AG (2008) Population trends of 48 common terrestrial bird species in Europe: results from the Pan-European Common Bird Monitoring Scheme. *Revista Catalana d'Ornitologia,* **24**, 4-14

Wechsler S (2018) Automating the analysis of territory mapping data in bird monitoring. UNOGIS-Paris Lodron-Universität Salzburg.

Weiss J, Schulze-Hagen K (2014) Viele Menschen–viele Vögel? Ornithologie und Vogelschutz in Nordrhein-Westfalen. *Charadrius,* **50**, 3-22

Wood S (2021) mgcv - Mixed GAM Computation Vehicle with Automatic Smoothness Estimation. *R package*, 1-323. https://doi.org/10.32614/CRAN.package.mgcv

Zuur AF (2012) *A beginner's guide to generalized additive models with R*. Highland Statistics Limited Newburgh, NY, USA.